DOI: 10.13009/EUCASS2017-191

The Oscillation Characteristics of Reactive Flow in the Hybrid Rocket Post Chamber

Sulha Lee, Changjin Lee**
**Konkuk University*
120, Neungdong-ro, Gwangjin-gu, Seoul 05029, Korea

Abstract

Recent experimental studies with visualizing flame images revealed that the occurrence of LFI (Low Frequency Instability <100Hz)) in hybrid rocket combustion is significantly related with the coupling of pressure and combustion fluctuations of around 500 Hz band in the post chamber. The combustion gas which containing the unburned fuel and small-scale vortices generated on the fuel surface flows into the post-chamber. Therefore, a complicated turbulent structure as well as additional combustion of the unburned fuel should take an important role of initiating the LFI process somehow. The purpose of this study is to implement chemical reaction together with the wall blowing effect in numerical calculation and to monitor the oscillatory characteristics of reactive flow in the post chamber.

1. Introduction

The hybrid rocket combustion shows a typical feature of LFI (Low Frequency Instability < 100Hz) under certain combustion conditions. Recently, Moon et al. [1] study had shown that the interaction between pressure (p') and combustion oscillation (q') of 500 Hz band in post-chamber is associated with the occurrence of LFI. Also, Park et al. [2] reported that 500 Hz band of pressure oscillation (p') was generated in associated with the change in flow characteristics in post chamber. However, the cause of the combustion oscillation (q' of 500 Hz band) and interaction between pressure and combustion oscillation of 500 Hz band are not fully understood and need additional study.

In previous studies, numerical calculation for non-reactive flow was done using LES methodology. And results showed that the appearance of 500 Hz p' is related to the generation of small size vortices in the combustion chamber [3]. By the way, small vortices were generated by the interaction of the fuel vaporization flow and the oxidant flow near the solid fuel wall. And these vortices could change microstructures of turbulence in the turbulent boundary layer near the combustor wall. Park et al. [4] also conducted a numerical calculation with LES for reactive flow modelled with simple chemical kinetics. Results show that the fuel vaporization flow was responsible for the generation of small vortices near the wall as already observed in the result of Na et al. [3], and the corresponding turbulent boundary layer was established with slight modifications in spatial and temporal distribution. Also it was reported that unsteady hot spots are formed and fluctuated vertically in the boundary layer. The results also show that unburned fuel is vaporized at the end of the fuel and enters into post chamber where the additional combustion occurs accompanying heat release oscillations. Although there is no detailed analysis of the effect of additional combustion on the flow characteristics, it is considered that the structure of the turbulent flow in the post combustion chamber seems to be very dependent to additional combustion. As a result, physical characteristics of p' and q' in terms of frequency band and oscillation phase will be influenced by inflow of small-scale vortices and additional combustion of unburned fuel in post chamber.

Generally, flow over BFS (Backward Facing-Step), which is very similar to the configuration of post-chamber, a recirculation zone appears beneath the shear layer. And the generation of the recirculation zone could influence the turbulent structures in BFS flow. Moin et al. [5] investigated the flow structures of the shear layer and the recirculation zone using the LES and DNS methodology. They identified three major parameters that are very crucial in determining temporal and spatial characteristics are Re (Reynolds number), ER (Expansion Ratio) and the turbulence characteristics of the inlet flow.

And temporal characteristics of the flow structures display very well-known two frequency bands of Strouhal number (St) = O (0.1) and O (0.3). Frequency characteristic of St=O (0.1) is corresponding to the appearance of recirculating vortex shedding. And velocity difference of shear layer at the inlet is responsible for the oscillations of frequency of St = O (0.3), which is usually called KH (Kelvin-Helmholtz) instability. Thus, the fuel vaporization and the formation of small size vortices entering into the post-chamber will significantly affect the modifications of turbulent flow structures.

However, Gohniem et al. [6] observed in their experiments that unsteady interaction between flame and vortex (vortices) were very active in the wake of the recirculation zone, also the heat release rate was found to oscillate

DOI: 10.13009/EUCASS2017-191

significantly. This result implies that the mutual interaction between flame and vortex in the wake region can affect the characteristics of combustion instability.
Another experimental study of bluff body combustion [7] shows very interesting results. A series of test was done to study the effect of combustion type (premixed or diffusion flame) on the stability characteristic by adopting different injection method; upstream fuel injection and closed couple injection. Results show any flow instability was observed with upstream injection. However, BVK (Bernard Von Karman) instability with large fluctuation amplitudes occurred in closed coupled injection. Therefore, the fuel injection method, which determines the physical way of fuel/oxidizer mixing, can be a critical parameter for stability behaviour. Also the change in spatial distribution of chemical reaction could affect the shear layer instability. Thus, the combustion instability and the unsteady change of the shear layer are highly correlated and the mutual interaction can determine the occurrence of the LFI.
Next, Fig. 1 shows the flame image in the post-chamber of hybrid rocket. Visualized image on the left shows stable mode of combustion and right one is unstable mode at the LFI [1]. It is well known that the recirculation zone beneath the shear layer shows a unique frequency characteristic of St=O (0.1) in a non-reactive flow [5]. However, Fig. 1 confirmed that additional combustion in post chamber may change the reaction distribution and alter the shear layer formation and unsteady feature including reattachment point oscillation depending on the stability mode, which may be affected by wake flow characteristics. Thus, the stability mode of combustion in hybrid rocket seems significantly to be related with shear layer oscillation and accompanied additional reaction.

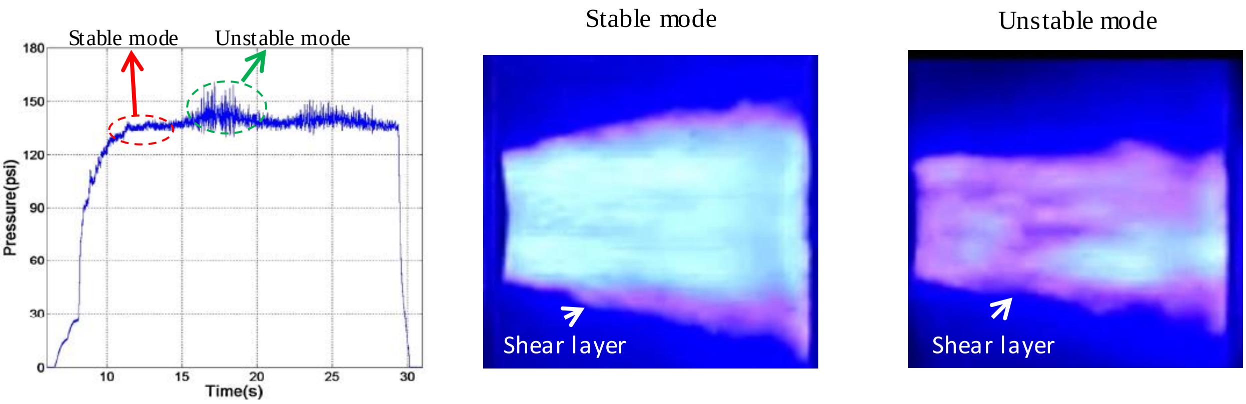

Figure 1: Flame Image of Post-Chamber

Small size vortices generated by the fuel evaporation in the hybrid rocket combustor enters into post-chamber and affect the generation of additional small size vortices in the shear layer. In addition, additional combustion of unburned fuel and the formation of the unsteady shear layer motion could be eventually interacted. Finally, understanding the correlation between flow structures and the combustion characteristics in the post-chamber would contribute to fully understand the occurrence of the LFI or the stable combustion mode. Therefore, main purpose of this paper is to investigate the change in flow structures including vortices distribution and temporal characteristic of fluctuations in post-chamber using LES calculation for the non-reactive flow. And we also investigate how the additional combustion in post-chamber affects the correlation between unsteady motion of the shear layer structure and additional heat release in post-chamber for reactive flow as well.

2. Numerical simulation

2.1 Governing equations for LES

A LES code has been developed for the study including preconditioning method, and compressibility effect in low Mach number domain. Normalized governing equations are continuity equation, Navier-Stokes equation, and energy equation that are filtered as in equation (1) where τ and t are time variables.

$$\Gamma \frac{\partial Q}{\partial \tau} + \frac{\partial W}{\partial t} + \frac{\partial (F_j - F_{vj})}{\partial x_j} = 0 \quad (1)$$

DOI: 10.13009/EUCASS2017-191

$$Q = \begin{bmatrix} p \\ u_i \\ T \end{bmatrix}, W = \begin{bmatrix} \rho \\ \rho u_i \\ \rho E \end{bmatrix}, F_j = \begin{bmatrix} \rho u_j \\ \rho u_i u_j + p\delta_{ij} \\ \rho u_i H \end{bmatrix} \quad \textbf{(2)}$$

$$F_{vj} = \begin{bmatrix} 0 \\ \tau_{ij} + \tau^*_{ij} \\ u_i(\tau_{ij} + \tau^*_{ij}) - q_j + (\mu + \sigma_k \mu_T \frac{\partial k}{\partial x_j}) - \dot{\omega}_k \end{bmatrix} \quad \textbf{(3)}$$

Here ρ and p are the filtered density and pressure, and u_i and u_j is velocity vectors for each axis in orthogonal coordinate system. Also, E is total energy, and H is total enthalpy, which is expressed as $H = E + p/\rho$. And τ_{ij} and τ^*_{ij} are laminar stress tensor and turbulent stress tensor respectively and these represent the total heat flux at each direction. $\dot{\omega}_k$ is chemical production rate of the kth species, but in this study chemical reaction term of energy equation is removed because non-reactive flow was solved. Also, SGS stress model used in the code incorporated Dynamic Smagorinsky model (DSM). A modified Roe-type flux difference scheme is also used which is suitable for LES. And viscous terms are calculated by central differencing. Time integration is done using a dual-time stepping method allowable for larger time-step size. LES code is composed to be clustered using MPI (message passing interface) for multi-block grid system by parallel processing. The solver is parallelized using an MPI-based domain decomposed strategy. The calculation usually took about 12 weeks with 16 CPUs.

2.2 Scalar transport equation

In this study, we used a passive scalar with the wall blowing in order to simulate the unburned fuel inflow. The Passive scalar is calculated from the following equation. A transport equation for the filtered mixture fraction, $\tilde{Z}$ is,

$$\frac{\partial \bar{\rho}\tilde{Z}}{\partial t} + \nabla \cdot \bar{\rho}\tilde{u}\tilde{Z} = \nabla \cdot \bar{\rho}(\tilde{D} + D_T)\nabla\tilde{Z} \quad (4)$$

where D_T is the turbulent diffusivity, modeled by dividing turbulent viscosity into turbulent Prandtl number ($D_T = \mu_T/Pr_T$). Density and velocity uses the value obtained from filtered conserved equation. With the Scalar transport equation is expected to be able to identify the characteristics of the mixing due to wall blowing through the distribution of a passive scalar.

2.3 Chemical Reaction Modeling

To take chemical reactions into account, an equilibrium combustion model is used [8]. The reversible chemical reaction is assumed to reach equilibrium state infinitely fast; thereby heat release of the final state can be directly exploited in the computation. Transport equation of a filtered conservative scalar is solved along with flow governing equations in LES. The conservative scalar is named as mixture fraction Z, defined as a following normalized formula when Y_F and Y_O are fuel and oxygen mass fractions and superscript zero (0) represents boundary values at fuel and oxidizer streams.

$$Z = \frac{\nu Y_F - Y_O + Y_O^0}{\nu Y_F + Y_O^0} \quad (5)$$

For a ν'_F (fuel) + $\nu'_{O_2} O_2 \leftrightarrow$ (product) reaction, stoichiometric oxygen-to-fuel mass ratio ν is defined as $\nu = \nu'_{O_2} W_{O_2} / \nu'_F W_F$. A transport equation for the filtered mixture fraction $\tilde{Z}$ is referred in (4) where D_T is the turbulent diffusivity, modeled by dividing turbulent viscosity into turbulent Prandtl number. Mixture fraction is discretized into 100 sample values, which are properly clustered near stoichiometric point. For each mixture fraction value, CHEMKIN subroutine is used to calculate equilibrium state solution, which is saved on a file as a lookup table. Equilibrium calculation routine also offers enthalpy at the final state that can be used to calculate reaction source for the energy equation $\widetilde{S_h}$. However, to simplify the routine, heat source is calculated using temperature difference between that the equilibrium states and current temperature, or $\widetilde{S_h} = C_p(\widetilde{T_e}(Z) - \tilde{T})$ where C_p is the heat capacity and $\widetilde{T_e}(Z)$ is the filtered temperature at the equilibrium state.
In LES, however, $\widetilde{T_e}(Z)$ is not identical to $T_e(\tilde{Z})$. A modeled sub-filter probability density function P(Z) is used to calculate filtered temperature for the equilibrium state for each computational cell [9].

DOI: 10.13009/EUCASS2017-191

$$\tilde{T}_e(Z)=\int_0^1 T_e(\xi)P(\xi)d\xi P(Z) \tag{6}$$

The filtered temperature $\tilde{T}_e(Z)$ is assumed to follow a beta distribution that bases on the first two moments. Smagorinky-type sub-filter variance model [10] is used to calculate second moment of the scalar while the first moment is directly obtained from the transport equation of $\tilde{Z}$. A lookup table is written in a separate file, which includes equilibrium temperature for 50 different variances for a given filtered mixture fraction. The combustion routine is integrated into the preconditioned compressible LES solver extensively used by the authors [11].
In the computation, methane (CH_4) reaction was implemented. A methane-air reaction mechanism was from GRI-Mech 3.0 [12]. Other computational details are identical to previous studies performed without a block case [3]. A cylindrical domain is discretized with 256, 64, and 128 cells in axial, radial, and azimuthal directions. A fully turbulent flow is generated through the periodic domain of ($-5 < x/D < 0$), which is followed by the fuel injecting part ($0 < x/D < 15$).
In reality, heat transfer from combustion to the fuel surface is the main source of fuel regression during the combustion, called pyrolysis. Thus, the amount of fuel pyrolysis rate is determined by the balance of heat transfer coming to the surface and heat absorptions from the surface associated with fuel evaporation and heat conduction. However, fuel (CH_4) was radially injected from the wall, with the linearly varying rate of 0% (at x/D=0) to 3% (at x/D=15) of the mainstream bulk velocity (23.3m/s). Reynolds number for the mainstream bulk velocity is 15,300. Decoupling of fuel regression rate from the combustion was proven as the effective method in studying near field flow dynamics in the solid propellant combustion. Even though this calculation frame is not suitable for evaluating fuel regression rate, flow motions of vortices generation and interactions leading to combustion stability can be properly described.

2.4 Numerical results in main chamber

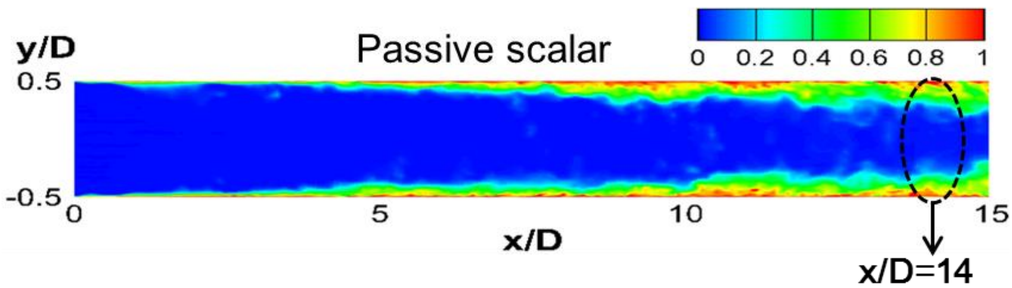

Figure 2: Distribution of passive scalar in the preliminary study

In the result of [4], a reactive flow in a combustion chamber of a hybrid rocket was analyzed to simulate gradually increasing vaporized fuel flow. Using a passive scalar was to predict the mixing of the fuel (passive scalar = 1) and oxidizer (passive scalar = 0). In this study, the non-reactive flow results in the combustion chamber with wall blowing were used for inlet conditions to the post-chamber. In addition, the passive scalar of unity was used as the boundary condition of wall blowing, and the passive scalar of 0 was used in the axial direction. In addition, the distribution of velocity and passive scalar at the location of x/D = 14 was used as the inlet condition of the post-chamber

2.5 Numerical domain and grid

As depicted in Figure 1, the pipe consists of two regions: inflow part ($-4 < x/h < 0$) and expansion part ($0 < x/h < 20$) where h is the step height of the post-chamber. The inflow part is added to provide realistic turbulence without any discontinuity to the main region of interest. The expansion region is applied to simulate effect of a regression process of solid fuel. The numbers of grid points used in inflow part to discretize the computational domain in axial, radial, and azimuthal directions are 64, 64, and 301, respectively, and the numbers of grid points used in expansion part to discretize the computational domain in axial, radial, and azimuthal directions are 301, 128, and 128, respectively. In radial direction, meshes are gathered using hyperbolic tangent function to capture near-wall flow accurately.

DOI: 10.13009/EUCASS2017-191

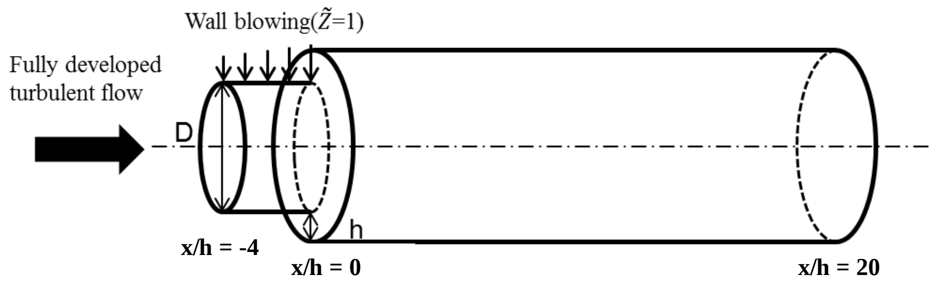

Figure 3: Numerical domain

A preconditioned compressible flow solver is used. A modified Roe-type flux difference scheme is also used which is suitable for LES and viscous terms are calculated by central differencing. Time integration is done using a dual-time stepping method to allow larger time-step size. A dynamic Smagorinky sub-filter model is used to closure LES terms. Additional information on the governing equations, boundary conditions and other methodologies used in the calculation is found in reference [13]. At the interface of inlet, information of velocity and passive scalar is passed through from the data of preliminary study.

Table 1: Calculation Case of the LES

	Case 1	**Case 2**	**Case 3**
Observation	No-wall blowing	Only wall blowing	Wall blowing and Chemical Reaction

Table 1 summarizes the calculation case in this study. Firstly, to investigate effect of the fuel vaporization flow in post-chamber, the results of case 1 and case 2 were used. And both case 1 and case 2 are non-reactive flow so only flow characteristics of wall blowing are analyzed. And to investigate the combustion characteristics of the unburned fuel in the post-chamber, case 2 and case 3 are compared. Only case 3 have reactive flow. Therefore, we will investigate the flow and combustion characteristics of the post-chamber in the hybrid rocket through these comparisons.

3. Results

3.1 Verification and Validation

Inlet with fully developed turbulent flow without wall blowing at step height Reynolds number of 5750 was simulated for validation purposes. Fig. 3 shows distribution of skin friction coefficient compared with value of [5]. Backward facing step with a similar expansion ratio (ER=1.2) and inlet Reynolds number based on step height (Re_h=5100) was calculated by DNS [5]. Overall value of skin friction coefficient was similar to the value of [5] although there are a little difference between computation and reference quantitatively. The point whose skin friction coefficient is zero represents a point of reattachment. In this study it was observed reattachment point represent 6.6 times of the step height. Reattachment length found in DNS results of backward facing step (BFS) was 6.28 times the step height [5]. The difference of reattachment length between computation and [5] is less than 5%. Fig. 4 is a diagram showing the comparison of the maximum turbulence intensity distribution in the axial direction between the computation and [5]. This also shows a similar trend as in the overall distribution of skin friction coefficient. The results in Fig. 3, 4 show that the code used in present study is valid to capture the important physical characteristics of the flow.

DOI: 10.13009/EUCASS2017-191

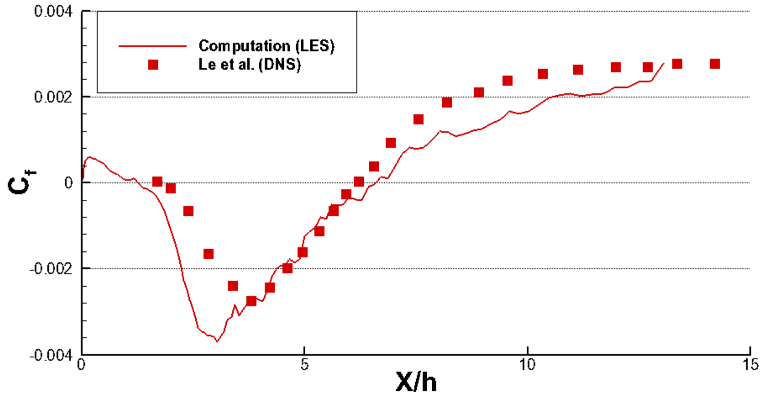

Figure 4: Distribution of skin friction coefficient

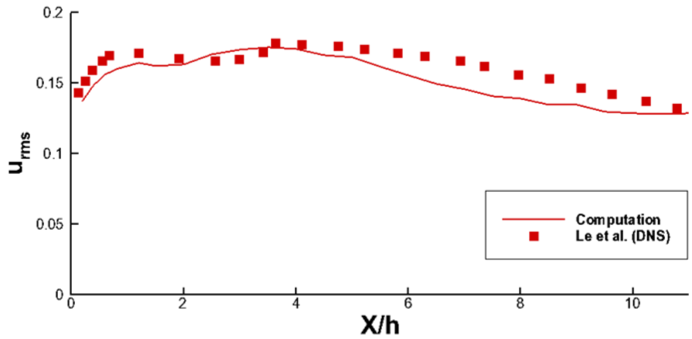

Figure 5: Maximum turbulent intensity value along the axial direction

3.2 Flow with wall blowing

In the hybrid rocket, the fuel vaporization flow influenced the turbulent structure change in the combustor and the generation of vortices near wall. Comparing to BFS flow, changed flow characteristics may occur when turbulent flows of combustor are introduced to post-chamber. We try to compare Case 1 and Case 2 which is the non-reactive calculation results to focus on the changes due to flow characteristics. Therefore, we analyzed the changes of flow structures as spatial and temporal characteristics.

3.2.1 Turbulent flow structure

Generally in the BFS, small-sized KH (Kelvin-Helmholtz) vortices are generated by the speed difference in the front of shear layer, and these vortices are expanded while moving to downstream. Fig. 6 shows the effect of the wall blowing in the post-chamber with distribution of z direction and x direction using lambda 2 (λ_2). Note that λ_2 is one of the useful methods to identify vortices in three dimensional flow fields. And λ_2 is mathematically defined as the middle eigenvalue of the symmetric matrix $S_2 + \Omega_2$ where S and Ω are the symmetric and anti-symmetric components of the velocity stress tensor. In the Fig. 6, the case of no-blowing (Case 1) shows that vortices are generated in the front of shear layer, but gradually disappearing toward downstream. It is judged to be KH (Kelvin-Helmholtz) vortices which are general characteristic in BFS. However in the case of only wall blowing (Case 2), a large amount of vortices are additionally generated and flowed to downstream. Particularly in the case of no-blowing (Case 1), it seems that vortices are generated in x/h=0.4 and gradually disappeared in x/h = 4. But in the case of only wall blowing (Case 2), the vortices don't gradually disappeared and these are maintained at x/h = 4.

DOI: 10.13009/EUCASS2017-191

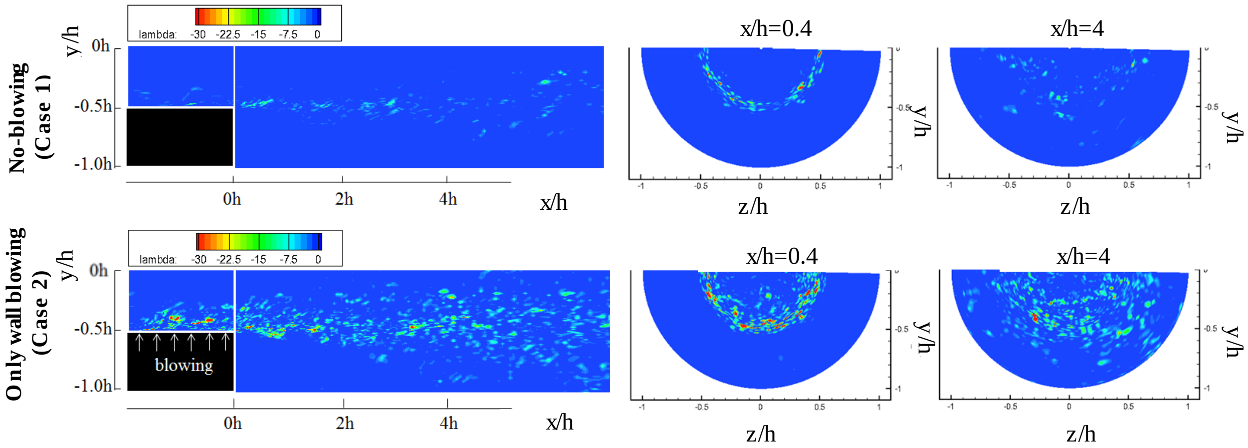

Figure 6: Contour of lambda 2 (λ_2)

Therefore, the vortices are generated near the wall of the combustor by wall blowing and the vortices flow into the post-chamber, which is considered to generate additional small-sized vortices in shear layer of post-chamber. The additional vortices change spatial distribution and these are thought to give a small scale variation in the shear layer of post-chamber.

3.2.2 Temporal change in flow characteristic

Table 2 shows the position of u′ (axial velocity fluctuation, $u = \bar{u} + u'$), and Fig. 7 shows the Strouhal number (St) of FFT analysis with u′ at each point. Strouhal number (St) is defined as $f \cdot L/U$ (f: frequency, L: length, U: mean velocity). In Fig. 7, the case of no-blowing (Case 1) showed a St = O (0.3) at x/h = 0.2, which is known as KH (Kelvin-Helmholtz) vortices in the front of shear layer. In addition, the oscillation characteristics of St = O (0.1) appeared at x/h = 5 and x/h = 10, which is also known as oscillation of the recirculation zone. [14] Therefore, the oscillation characteristics in the case of no-blowing (Case 1) are judged to general BFS flow characteristics.

Table 2: Calculation Case of the LES

point	Position
x/h = 0.2	(0.2, 0.5, 0)
x/h = 5	(5, 0.5, 0)
x/h = 10	(10, 0.5, 0)

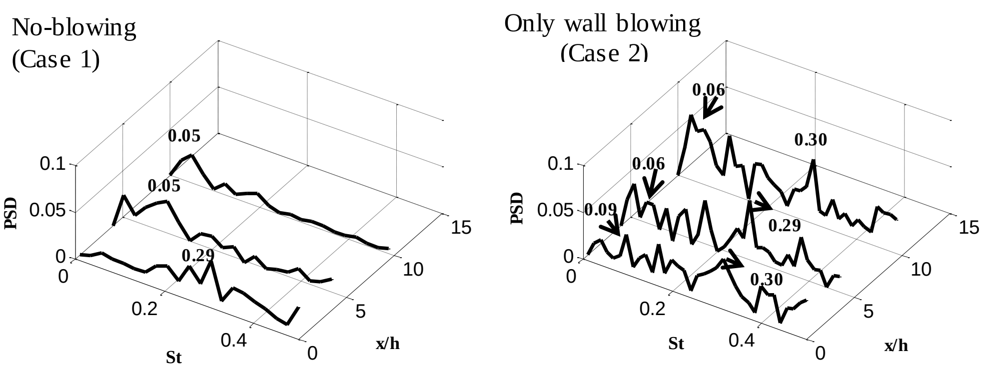

Figure 7: Strouhal number (St)

DOI: 10.13009/EUCASS2017-191

However, in the case of only wall blowing (Case 2) of Fig. 7, the oscillation of St=O (0.3) appeared at x/h = 0.2 and appeared additionally at x/h = 5 and x/h = 10. Additional vortices appeared at the front of shear layer and gradually disappeared at downstream when there is no wall blowing. However, in the case of wall blowing (Case 2), additional vortices did not disappear and continued to move downstream. Therefore, it is considered that the generation of St=O (0.3) at downstream appeared due to the additional vortices. Note that the oscillation frequency of St=O (0.3) is corresponding to a dimensional frequency of 490 Hz, which approximately coincides with a measured frequency band of 500 Hz. In addition, the case of only wall blowing (Case 2), St=O (0.1) occurred at x/h = 0.2. Therefore, unlike the case of no-blowing (Case2), it is suspected that the movement of the recirculation zone may occurred at x / h = 0.2. As a result, it is judged that the fuel vaporization flow gave a small scale variation in the post-chamber. And recirculation zone movement region seem to be expanded to upward.

3.3 Reactive flow in post-chamber

In the hybrid rocket, the fuel vaporization flow generated additional vortices and the combustion region of the combustor is separated from the wall due to the change of the turbulent boundary layer. In addition, at the end of the combustor, unburned fuel flows into the post-chamber and additional combustion seems to be occurred. The area where the additional combustion occurs in post-chamber has not been observed in previous study. However, it is predicted that the combustion affect to combustion characteristics of post-chamber. And it is possible that the unsteady motion of the shear layer is appeared. Therefore, the combustion characteristics of the unburned fuel in the post-chamber will be examined.

3.3.1 Mean velocity

Fig. 8 shows the length of the recirculation zone using streamline. Generally, when combustion occurs, the length of the recirculation zone becomes shorter and the thickness of the shear layer becomes thicker. Comparing the case of only wall blowing (Case 2) and the case of wall blowing and reaction (case 3), recirculation zone becomes shorter from 9.12h to 7.82h. In Case 3 of Fig. 8, the length of the recirculation zone is shortened by combustion. It can be seen that the change in the length of the recirculation zone occurring in the post chamber coincides with the combustion effect. It is suspected that the change in turbulent boundary layer, the thickness of the shear layer and the motion of the recirculation zone will be affected by the change in length of the recirculation zone. Therefore, the effect of combustion on the turbulence structure of the shear layer is examined.

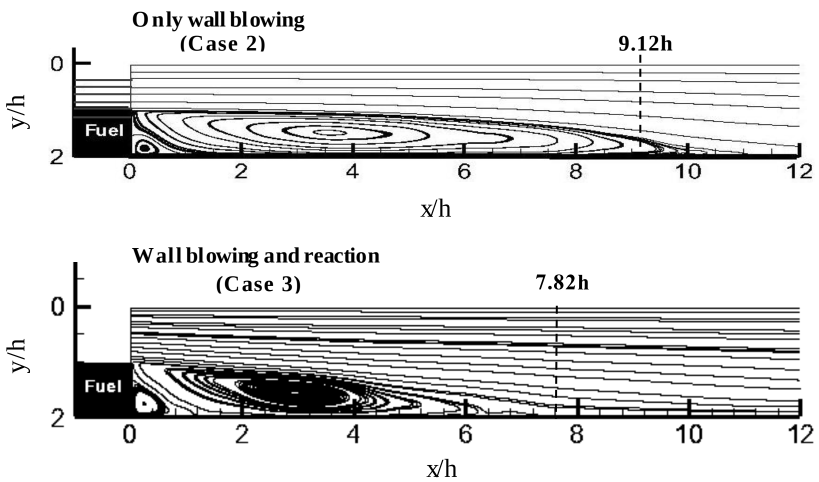

Figure 8: Mean profile of Recirculation zone

3.3.2 Temporal change in flow characteristics

Fig. 9 shows the results of the vortices generation in the shear layer using lambda 2 (λ_2). As a result, small-sized vortices introduce to post-chamber and these vortices generated additional small scale vortices in the shear layer despite of combustion. And additional vortices are moved to downstream like Case 2.

DOI: 10.13009/EUCASS2017-191

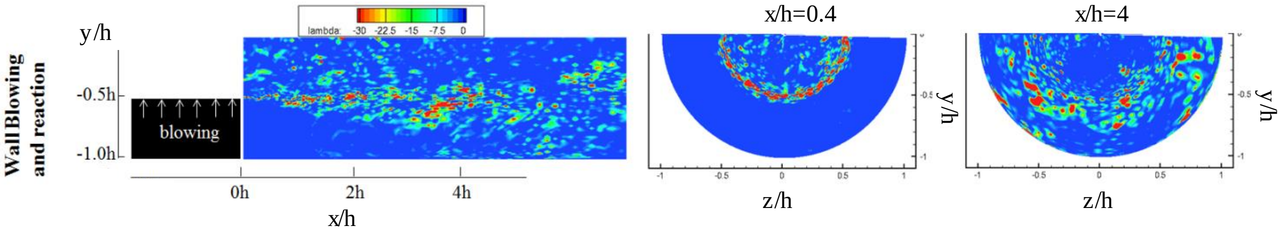

Figure 9: Contour of Lamda 2 (Case 3)

Combustion is causing volumetric expansion and forming the characteristic of large-scale. [15] So generally, the vortices are expanded and disappeared by the effect of combustion. However in the case of the wall blowing and reaction (Case 3), vortices did not expand and moved to downstream. And it shows characteristic of the additional combustion which similar to change of Case 2. So in the post-chamber, additional combustion did not change the small-sized vortices in shear layer. But additional combustion may affect to shear layer characteristics of large scale unlike Case 2.

3.3.3 Additional reaction by unburned fuel

Fig. 10, 11 and 12 are distribution of the u′ and scalar and temperature. First, Fig. 10 show the distribution of u' in x-direction. In the figure, the distribution of u 'is asymmetric in the shear layer. This may seems to be related to the additional combustion and the hot spots which are introduced of combustor. The Fig. 11 shows the distribution of scalar which means the mixture fraction. Scalar = 1 represents the fuel and scalar = 0 represents the oxidant. The unburned fuel introduced by the combustor shows the following distribution in the post-chamber. The Fig. 12 shows temperature distribution in the post-chamber. Temperature distribution is related to reaction region by the unburned fuel. In the figure, hot spot which is introduced in combustor flows into post-chamber and also generates in the downstream by additional combustion. Therefore, it seems that the combustion characteristics of the post- chamber generate the hot spot and the hot spot region move to downstream with unsteady motion.

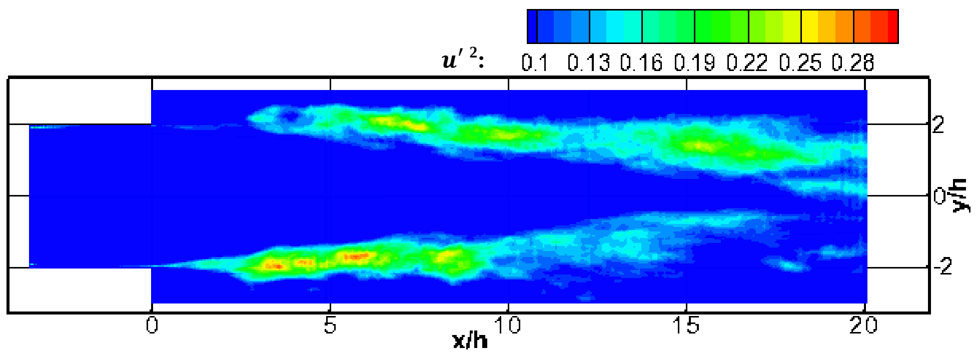

Figure 10: $u'^{\,2}$ distribution; wall blowing and reaction (case 3)

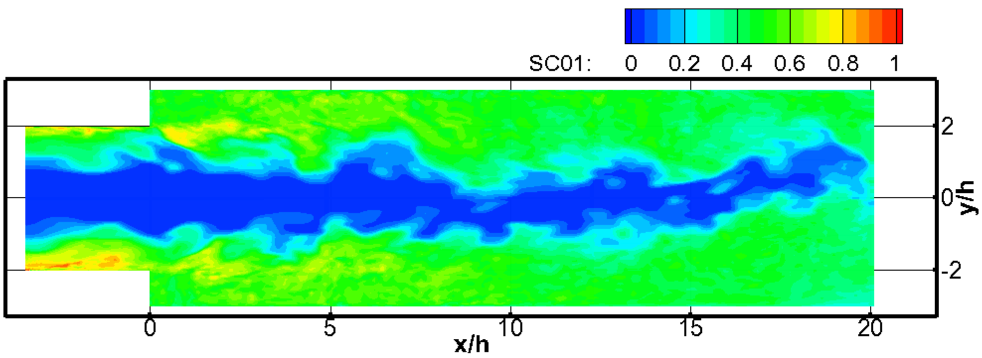

Figure 11: Scalar distribution; wall blowing and reaction (case 3)

DOI: 10.13009/EUCASS2017-191

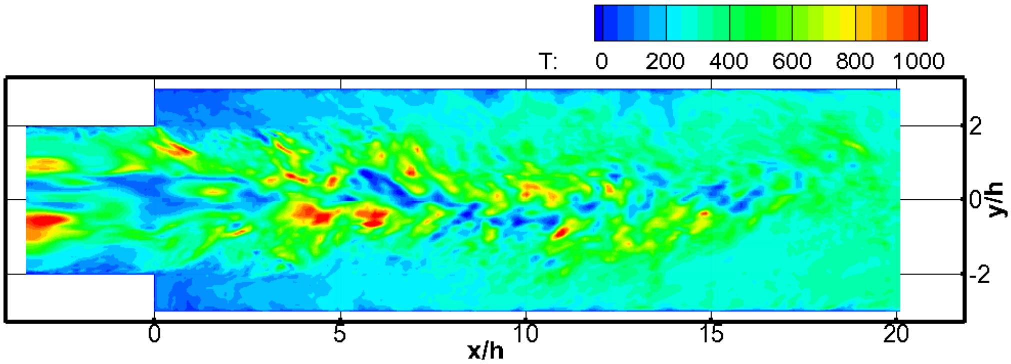

Figure 12: Temperature distribution; wall blowing and reaction (case 3)

3.3.4 Unsteady motion of shear layer

Fig. 13 shows the results of additional vortices movement in the shear layer of post-chamber using Q-criterion. Since vortices are considered to be an important research parameter, there is a need to introduce a method of observing vortices. So Q-criterion is used. As a result, in the case of only wall blowing (Case 2), small-sized additional vortices are generated in shear layer. However, the movement of the shear layer did not occur extensively. In the case of wall blowing and reaction (Case 3), the vortices appeared as large motion in the shear layer with time. So additional combustion results to unsteady motion of shear layer.

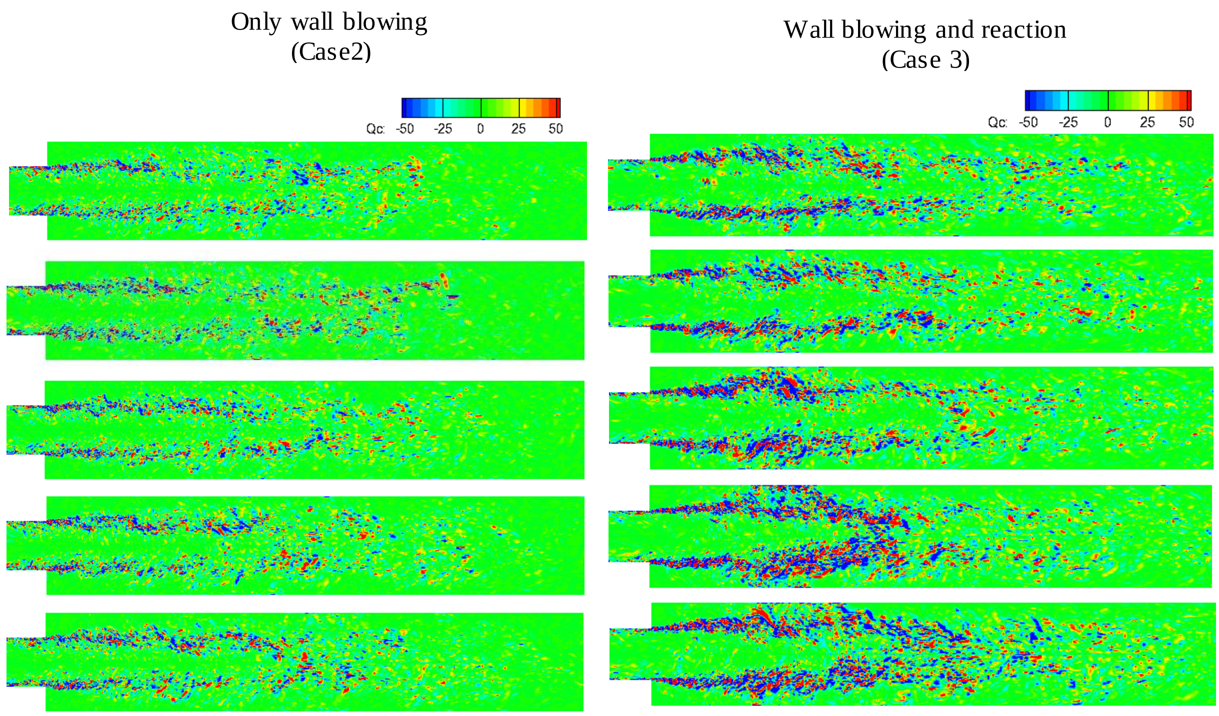

Figure 13: Unsteady motion of Q-criterion distribution

DOI: 10.13009/EUCASS2017-191

4. Conclusion

To understand the spatial distribution and temporal characteristic of turbulent flow including small size vortices in post chamber, numerical calculation has been done for reactive flow to investigate flow structures in shear layer along with additional combustion of unburned fuel from the main chamber using LES methodology. As a result, modified turbulent flow structure containing small size vortices in main chamber induces subsequent unsteady motion and different axial distribution of small-sized vortices along the shear layer. Results also revealed that additional small vortices along the shear layer were pushed further to downstream. Furthermore, additional combustion of unburned fuel is intensively observed near the front part of the shear layer, which causes small-sized vortices to continue to appear and to disappear in the shear layer, leading to downstream.
However, when the high temperature spots generated in the main combustion chamber flows into the post combustion chamber, the unsteady motion of turbulent structure appears, and a very large fluctuating motion begins to appear along the shear layer. The appearance of large scale unsteady motion along the shear layer seems to be very similar to that of BVK motion observed in the reference [7].
Thus, the spatial and temporal characteristics of turbulent flow and combustion in the post-chamber are judged to be determined by the generation of small size vortices and additional combustion of unburned fuel. Nonetheless, the exact mechanism leading to LFI is not yet understood. And further investigations are needed for the reactive flow in the post-chamber.

Acknowledgments

This work was supported by the National Research Foundation (2015R1D1A1A01058070) in Korea.

References

[1] Moon, Y. J., and Lee, C. 2016. Flame interaction with shear layer flow in the post-chamber of hybrid rocket. *J. Korean Society for Aeronautical & Space Sciences*. 44:585-592.
[2] Park, K. S., and Lee, C. 2015. Low frequency instability in laboratory-scale hybrid rocket motors. *Aerospace Science and Technology*. 42:148-157.
[3] Na, Y., and Lee, C. 2009. Large eddy simulation of flow development in chamber with surface mass injection, *Journal of Propulsion and Power*. 25:51-59.
[4] Park, C., and Lee, C. 2015. Vortices generation in the reactive flow on the evaporative surface. *Journal of Mechanical Science and Technology*. 29: 563-570.
[5] Le, H., Moin, P., and Kim, J. 1997. Direct numerical simulation of turbulent flow over a backward-facing step. *Journal of Fluid Mechanics*. 330:349-374.
[6] Murat, A. H., Ghoniem, F. 2009. Flame–vortex interaction driven combustion dynamics in a backward-facing step combustor, *Combustion and Flame*. 156:1111–1125.
[7] Lovett, J. A., Cross, C., Lubarsky, E., and Zinn, B. T. 2011. A Review of Mechanisms Controlling Bluff-Body Stabilized Flames with Closely-Coupled Fuel Injection. In *ASME 2011 Turbo Expo: Turbine Technical Conference and Exposition*. 1275-1287.
[8] Coronetti, A., and Sirignano, W. A. 2013. Numerical analysis of hybrid rocket combustion, *Journal of Propulsion and Power*, 29: 371-384.
[9] Peters, N. 2000. Turbulent combustion. *Cambridge University Press*, Cambridge, UK
[10] Cook, A. W., and Riley, J. J. 1994. A subgrid model for equilibrium chemistry in turbulent flows, *Physics of Fluids*. 6: 2868-2870.
[11] Pierce, C. D., and Moin, P. 1998. A dynamic model for subgrid-scale variance and dissipation rate of a conserved scalar, *Physics of Fluids*, 10: 3041-3044.
[12] Koo, H., Mon, K., and Lee, C. 2012. The effect of a block on the flow oscillations near the fuel sur-face with wall blowing, *48th AIAA/ASME/SAE/ASEE Joint Propulsion Conference and Exhibit*, *Atlanta*, Georgia, USA 2012-4108.
[13] Aider, J. L., Danet, A., and Lesieur, M. 2007. Large-eddy simulation applied to study the influence of upstream conditions on the time-dependant and averaged characteristics of a backward-facing step flow. *Journal of Turbulence*. 8:N51.
[14] Rhee, G. H., and Sung, H. J. 2000. Numerical prediction of locally forced turbulent separated and reattaching flow. *Fluid Dynamics Research*. 26: 421-436.
[15] Fureby, C. 2000. A computational study of combustion instabilities due to vortex shedding. *Proceedings of the Combustion Institute*. 28: 783–791.